Entropy, pattern entropy, and related methods for the analysis of data on the time intervals between heartbeats from 24-h electrocardiograms

J. J. Żebrowski,[1] W. Popławska,[2] and R. Baranowski[2]
[1]*Institute of Physics, Warsaw University of Technology, Warszawa, Poland*
[2]*National Institute of Cardiology, Warszawa, Poland*
(Received 18 March 1994)

Sequences of the time intervals between heartbeats—medically termed *RR* intervals—extracted from 24-h electrocardiogram recordings are examined as three-dimensional return map images. The recordings were made in humans by means of the medically widely used portable electrocardiograph (Holter system). A time window measured in the number of heartbeats is used and different types of behavior are classified. Bifurcations between the types of dynamics of the heart are noted and a form of intermittency is found. An alternative quantitative measure—a form pattern entropy of the return map image—is defined that characterizes the dynamics of the *RR* interval sequence. It is shown that this is a measure of the degree of ordering of the *RR* interval sequence and as such it is a good novel medical diagnostic tool for analyzing heart rate variability which distinguishes between illness and health where other diagnostics fail.

PACS number(s): 87.10.+e, 05.45.+b, 87.80.+s

I. INTRODUCTION

Over the past decade strong evidence has been found that the dynamics of the heart has at least a dominantly deterministic nature [1–3]. The complexity of the behavior of the heart as seen through surface electrocardiograms (ECG) in humans is now attributed to the nonlinearity of the nervous system regulating the heart [3]. Simultaneously, many questions have been posed (and not all have been answered) whether the well established methods of nonlinear dynamics are able to cope with the analysis of the ECG signal in general and with heart rate variability in particular. There seems to be a consensus that phase trajectory portraits and return maps are sensitive tools [4,5] which do give insight into the subtle changes in the dynamics of the heart such as bifurcations [4,6]. On the other hand, standard nonlinear dynamical tools such as correlation dimensions [4] and $f(\alpha)$ curves [7,8] may cause problems. These methods require a rather large number of data points on input, but also they assume stationarity of the data. This may be in conflict with the inherent nonstationarity of the ECG, which is often made during exercise stress tests or simply spans a long time, e.g., 24 h. In this context, methods which calculate pointwise correlation dimensions [9,10] should be considered an important advance in the analysis of ECG data.

The analysis of ECG data may be divided into two basic areas. In morphological analysis the shape of electrical pulses measured is examined and information on the processes which occur mainly within the heart during each beat is sought. On the other hand, in the complimentary type of ECG analysis the time distance between heartbeats—the *RR* intervals—is measured and information on the processes which control heart action is sought.

In the studies performed using various analytical methods of *RR* interval analysis [11,12] two opposite approaches are often assumed. Either a short recording of the data in specific medically controlled conditions is made (short term recording) or the whole 24-h data set is analyzed (Holter method). In the latter case, the one studied here, the patient wears a miniature recording device which enables him to perform all actions the state of his health permits. Many attempts have been made to try to assess the health of the patient by looking at global, statistical time domain characteristics of the whole 24-h period of data [11]. Medically interesting short stretches of the recording are often singled out for additional power spectral analysis or for short time domain (statistical) analysis. Similarly, attempts have been made of nonlinear dynamical analysis of *RR* intervals, e.g., the shape of two-dimensional images of the *RR* intervals maps compiled from the whole 24-h recording has been associated with the state of health [5], and quantitative measures such as the correlation dimension [4,6] and $f(\alpha)$ curves [8] have been calculated for *RR* interval sequences. Since the dynamics of the heart rate variability is a reflection of neurohumoral activity, bifurcation analysis of three-dimensional images of *RR* interval return maps and a quantitative measure called approximate entropy [13] of *RR* intervals has been used to monitor the behavior of both the patients and the therapists during psychotherapy [14,15].

The purpose of this paper is to discuss ways to analyze the dynamics of *RR* intervals in 24-h Holter ECG recordings. Three-dimensional images, formed by way of the theorem of Takens [16], of medically representative cases of such recordings are presented. A time window is used to scan through the 24-h recording and bifurcations in the data are discussed. Entropy of the *RR* sequence is calculated and a new quantitative measure of the complexity of three-dimensional images of the *RR* sequences—a form of pattern entropy–is defined. This

measure is shown to distinguish between different cases of pathology and health in medical circumstances such that the frequency and time domain analysis of the *RR* intervals often fails.

II. DATA

Holter ECG 24-h tapes of both healthy individuals and cases of heart disease with the highest risk of sudden death were analyzed by commercial software (Del Mar Avionics 563 Strata Scan). The data were sampled at 128 Hz and the time distance between consecutive *R* peaks (the *RR* intervals) was extracted. No special filtering was used, but *RR* intervals larger than 2000 ms were treated as artifacts and ignored. Each 24-h sequence of *RR* intervals studied was 80 000–125 000 data points long.

The main body of the patient population of which the data are quoted here consisted of 15 persons (14 male and 1 female), 41±8 yr of age, who belonged to the highest cardiological risk group and who had experienced cardiac arrest due to ventricular fibrillation (14 patients) or asystole (1 patient). Ventricular fibrillation was a complicating factor in the coronary disease of 11 patients from this group, one person had valvular heart disease, and one had arrhythmogenic right ventricular disease. For two cases in this group, no apparent heart disease was found, except for recurrent ventricular fibrillation. Three patents had their arrhythmic event occur while wearing the Holter device; one of them died. Two other patients subsequently died suddenly, while one has recurrence of ventricular arrhythmia. Following standard medical practice, each of the 15 persons from the high risk group had an age, sex, and disease status matched pair serving as the control. Only due to such meticulous one to one matching of pairs could the statistical correlation between the two groups be meaningful. For statistical comparisons the paired *t*-student test was used.

III. IMAGING

In most problems analyzed by nonlinear dynamical methods not all the variables needed to construct the phase space trajectory of the system are available. Instead the Takens delay-coordinated reconstruction of the phase space trajectory [16] is made using only a single time series of a single variable of the system. If the full *QRS* complexes of the ECG signal are treated as the raw data, then extracting the *RR* intervals amounts to taking the time differences between points on a Poincaré section of the full trajectory in the phase space of the system.

Three-dimensional images of the return map $\Delta_{RR}(i+2\tau)$ versus $\Delta_{RR}(i+\tau)$ and $\Delta_{RR}(i)$, where i is the index of the *RR* interval, τ is the delay, and Δ_{RR} is the *RR* interval length, were formed from the *RR* interval data. As usual, the choice of the time delay is difficult. Often rather sophisticated methods—the first minimum of mutual information or of the autocorrelation [17]—are used for this purpose. Calculating mutual information is a problem in itself, especially since it is expected that 24-h Holter ECG data may be nonstationary. The same applies to the autocorrelation or the autocovariance function. When calculated from the usual basic definition, the autocorrelation function of *RR* interval data, except for rare cases, was found to be a nonmonotonically decreasing positive function. We found that the Takens delay for the data presented here should be in the range from 1 to 9 beats as determined by the first minimum of the autocorrelation function. The first minimum of the autocovariance function was situated at 1–20 beats and the first zero crossing was situated at 20–150 beats depending on the medical case and on the length of the series taken for the calculation. The longer the series used in the calculation the less visible the local minima occurring before the first zero. Since the features of both the autocorrelation function and the autocovariance function depended strongly on the length of the time window for which they were calculated, we found it a very imprecise criterion to determine the delay for phase space reconstruction on the basis of these functions. Also, the purpose of attempting to develop the methods described in this paper is to avoid the calculation of the Fourier spectrum of the *RR* intervals (through which the autocorrelation function may also be found) as this creates well known severe problems [12]. As a rule of thumb, the delay time should not be too large so that valuable characteristics of the phase space trajectory are not lost in the stretching and folding process which occurs during the time evolution of the system. Because the *R* peaks in the PQRST sequence of the ECG signal are a full cycle of heart action away, there is a tendency to use $\tau=1$ [5]. On the other hand, the larger the value of τ the more independent the variables $\Delta_{RR}(i+n\tau)$, with $n=0,1,2,\ldots$ and i the *RR* interval index, become. Furthermore, visualization of characteristic features of the reconstructed trajectory is enhanced with larger τ since the image is stretched further away from the diagonal of the figure. In three dimensions, we found that an integer delay $\tau=2$ was adequate, but fixed time delays as large as 12 s (equivalent to an integer delay from 12 to 30 beats) have also been used by other groups [3,18].

Several examples of 24-h recording of Holter ECG data in the three-dimensional return map image are shown in Figs. 1–3. Case H.R.N. [Fig. 1(a)] and case C.H.M. [Fig. 1(b)] were considered healthy by standard medical practice. Patient G.D.S. [Fig. 2(a)] had symptoms of ventricular arrhythmia due to dilated cardiomyopathy, while F.A. [Fig. 2(b)] is a good example of atrial fibrillation which is characterized by a completely irregular *RR* sequence. Note that even though each image in Figs. 1 and 2 consists of over 10^5 points, small islands exist at the fringes of the images which the system does not visit. Figure 3 depicts two recordings of the same patient D.W.D.: (a) 18 h before cardiac arrest due to ventricular fibrillation and (b) 1 yr after cardiac arrest and subsequent medication. It can be seen that it is possible to immediately distinguish between the dynamics of *RR* intervals of healthy individuals (Fig. 1) and that of the severely ill patients seen in Figs. 2 and 3(a). But, in this the 24-h picture, distinguishing between, e.g., ventricular arrhythmia [Fig. 2(a)] and atrial fibrillation [Fig. 2(b)] is difficult. Note that, medically, these are completely different conditions. Furthermore, one would want to be able to assess whether patient D.W.D. remains in danger

of a repeat of cardiac arrest, i.e., whether there is a measurable difference between the data of Figs. 1 and 3(b).

From the medical point of view, there are obvious reasons by the Holter ECG data recorded during the day are different from those taken during the night's rest. It has also been noticed in the past that heart action undergoes various bifurcations [18,4]. These bifurcations can be made visible when not too many points are plotted on the *RR* return maps, i.e., when the maps are viewed through a time window. Because the heart rate changes substantially and rapidly, we found it convenient to define such a window in the number of beats (integer time) rather than in a fixed number of seconds. To be able to study bifurcations occurring during heart action, the computer program had the capability to connect, on demand, subsequent points on the map by a line. Such an imaging of the dynamics of the *RR* intervals has been used in the past [14,15,18].

We classified the principal types of behavior found in our Holter data according to the motion of consecutive points on the computer screen. Figure 4(a) is an example of what we called radial behavior where there is an alternation of short and long *RR* sequences. Figure 4(b) depicts the opposite type, i.e., spiral behavior. Each of the types may be the sole type of behavior for a given individual. For example, spiral behavior is most often seen in healthy individuals, while radial behavior is typical for arrhythmias, but it is not identified uniquely with this pathology and may occur in other ailments. Bifurcations may occur from one type of behavior to the other. An example of such behavior is depicted in Fig. 5. Prior to the image seen in this figure a long sequence of spiral behavior occurred. In the sequence of 200 heart beats (3 min, 2 s) in Fig. 5, spiral behavior was still dominant (mostly small spirals, forming the core of the figure), but the occasional bursts of radial behavior created the characteristic crosslike shape. This behavior seems to be some form of intermittency. The whole 24-h recording

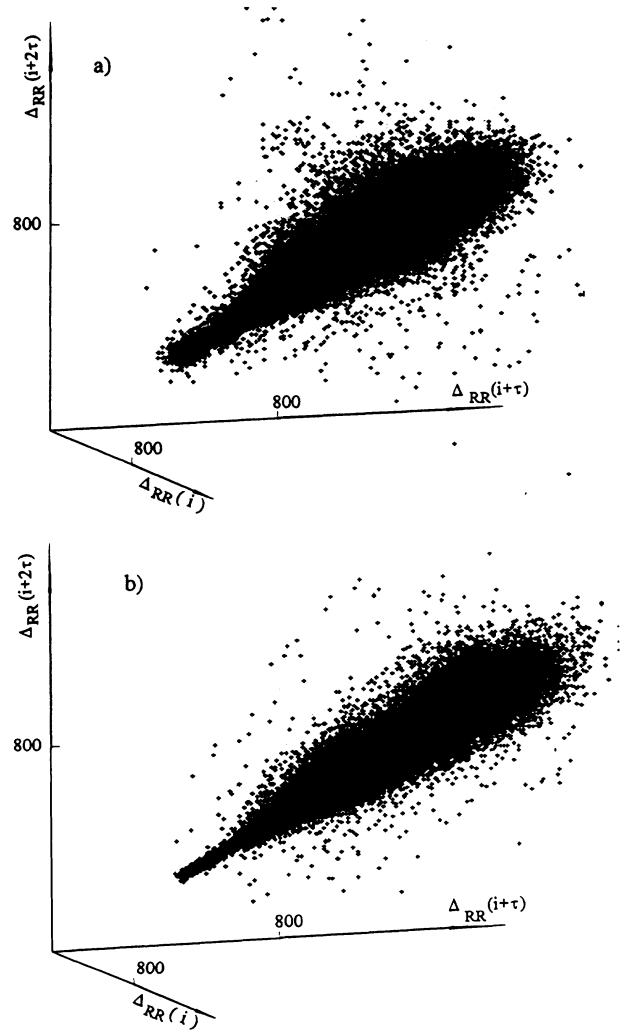

FIG. 1. Three-dimensional images of *RR* interval return maps with $\tau=2$ calculated from 24-h Holter ECG recordings of two individuals considered healthy: (a) patient H.R.N. and (b) patient C.H.M.

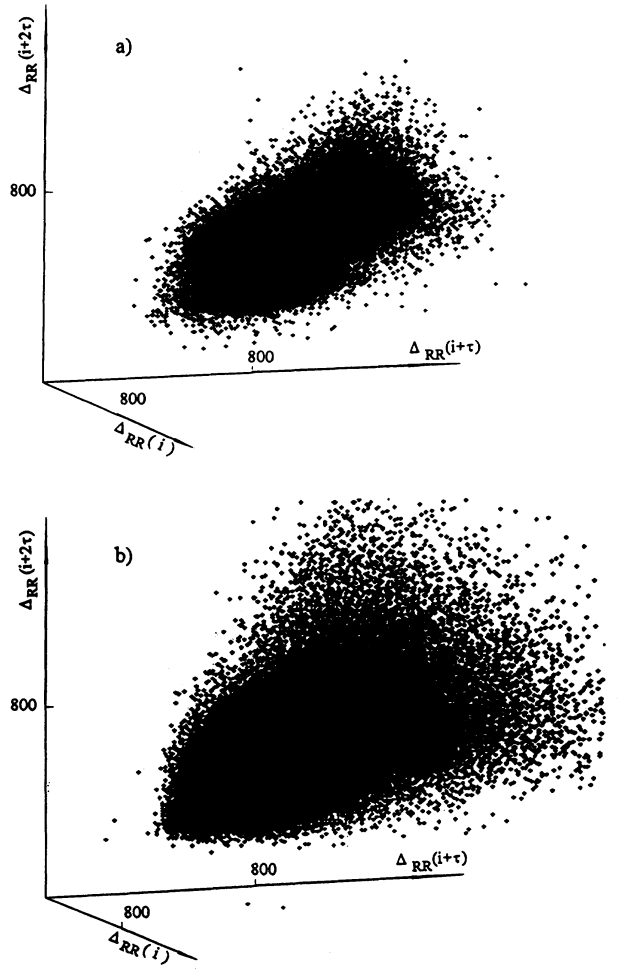

FIG. 2. Three-dimensional images of *RR* interval return maps with $\tau=2$ calculated from 24-h Holter ECG recordings of a case of (a) ventricular arrhythmia G.D.S and (b) atrial fibrillation F.A.

for this case of hypertrophic cardiomyopathy consists of bifurcations and reverse bifurcations between sequences of radial and spiral behavior. We stress that term "bifurcation" is used here on the basis of the rather weak argument that the changes in dynamic behavior occur sharply in time and that they show some geometrical similarity to bifurcations of low-dimensional map theory. If one accepts that the sharp transitions in the dynamics of the *RR* intervals series are true bifurcations, then one may conclude that a hitherto unknown control parameter exists which changes as the *RR* interval series progresses. In any case this term has been applied to *RR* interval data before [4,18] in similar circumstances.

The three-dimensional images of *RR* intervals discussed here are, by construction, return maps. Obviously, these maps are much more complex than the quadratic or circle maps most often analyzed in the literature. However, there are cases when the usually complex return map of *RR* intervals bifurcates to a much simpler state. The initial 30 min of the *RR* intervals recorded from patient C.G.N. were dominated by spiral behavior. Then a bifurcation occurred to an extremely periodic state (Fig. 6), which lasted for about 50 min with slight changes in the number of points in a given island. After returning to a more normal looking, spiral dominated trajectory shape, 10 min later this patient died suddenly due to asystole. Note that the analysis of heart rate variability based on standard methods including power spectrum analysis showed no substantial abnormalities in this case. Bifurcations to such complex periodic behavior are not uncommon and do not necessarily signify an immediate cardiac arrest. Note also that the island structure of the map in Fig. 6 is in reality a limiting case of an instance of radial behavior which is, however, extremely stable in time and especially well ordered.

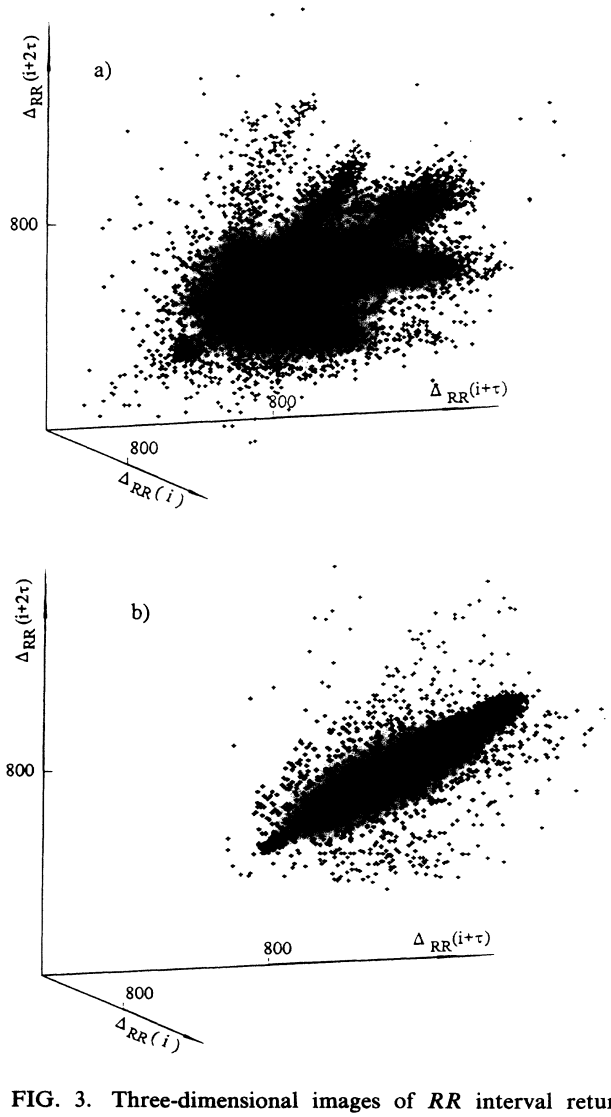

FIG. 3. Three-dimensional images of *RR* interval return maps with $\tau=2$ calculated from 24-h Holter ECG recordings of the same patient (a) before cardiac arrest and (b) 1 y after.

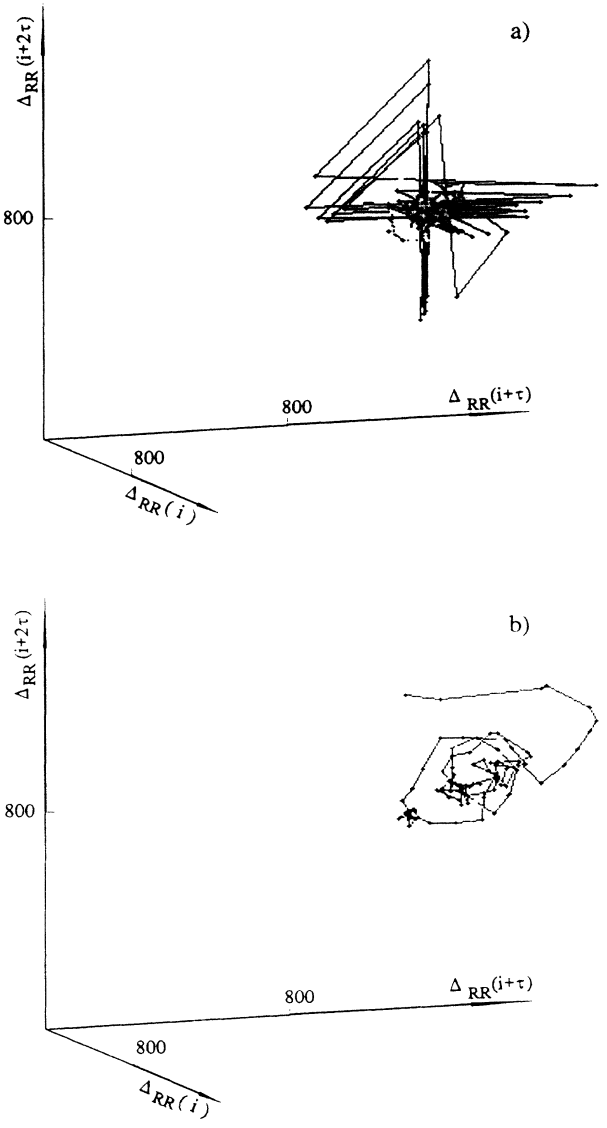

FIG. 4. Types of *RR* interval sequences: (a) radial behavior and (b) spiral behavior.

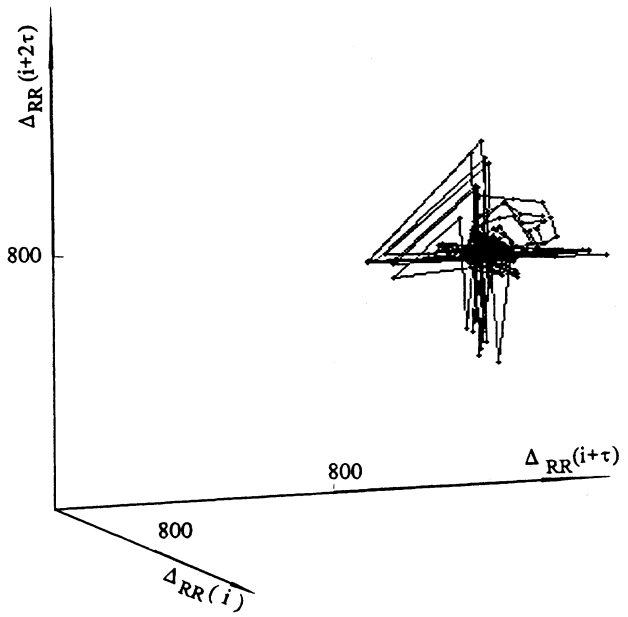

FIG. 5. Intermittent bursts of radial behavior during a predominantly spiral *RR* interval sequence.

IV. ENTROPY OF *RR* INTERVALS

RR intervals have been analyzed in the past by techniques based on the use of histograms [11]. Pincus, Gladstone, and Ehrenkranz [13] used approximate entropy (a form of the Kolmogorov K_2 entropy) to measure the differences between *RR* sequences (cf. [14,15]). Figure 7 depicts typical histograms of 400-beat-long *RR* sequences taken from 24-h Holter recordings. To assess quantitatively the differences between such histograms we calculated the entropy of such an *RR* sequence by using

$$S=-\sum_{k=1}^{N} p_k \ln p_k \ , \tag{1}$$

where N is the number of bins of the histogram and p_k is the probability of obtaining the *RR* interval length Δ_{RR} corresponding to the kth bin of the histogram. The probability p_k is simply the value of the histogram at the kth bin when the histogram is normalized by the total number of beats in the given *RR* sequence. Since the sequence of *QRS* complexes was digitized with a 7.5-ms sampling time, to construct the histograms with optimal computing time we used a bin size of 25 ms, somewhat larger than the sampling error.

When the values of S measured for different cases of 24-h *RR* interval sequences were compared, the results were rather discouraging. The values of S were very close (from 2.7 to 3.5 in arbitrary units) for cases which were evidently vastly different when viewed as the three-dimensional return map. For example, a healthy individual may have the entropy of the 24-h *RR* interval sequence 2.95, while a bad case of cardiomyopathy would yield 2.96 and another gave 2.98. The entropy of the full 24-h *RR* interval sequence of another healthy individual H.R.N. [Fig. 1(a)] was found to be 3.36, which could easily be confused with the results found for cases of arrhythmia (3.08–3.83) or cardiomyopathy (2.65–3.38).

An important improvement was obtained when a time window of length N scanning through the whole 24-h sequence was introduced into the procedure and Eq. (1) was used to calculate the entropy for the window. The resultant window entropy S_w was compared with cumulative entropy S calculated using (1) and counting N as the number of *RR* intervals from the beginning of the sequence to the local time value. Note that there does not seem to be a clear-cut way of establishing the length of the time window to use. On the one hand, such a window may not be too short (e.g., less than 30–50 beats) so as to maintain good statistical properties of the normalized histogram used in (1). On the other hand, for a time window which is overly long (e.g., over 5000 heartbeats long) the patient wearing a Holter apparatus may undergo many vastly different physical actions rendering such long time averaging meaningless. Moreover, the values of the window entropy S_w and of cumulative entropy S converge for large window sizes. For the purpose of this study, the window length was assumed to be 400 beats, which, depending on the situation and on the patient studied, corresponds to 3–6 min of real time. Windows of the order of 100 beats in length have also been studied, showing promising characteristics of the details of the *RR* sequences, and will be reported on in the future.

Examples of the first 4 h of the one-dimensional entropies as functions of time are shown in Fig. 8 for the healthy individual C.H.M. and in Fig. 9 for patient B.H.D., who has undergone several cardiac arrests over the past 5 yr (he is now equipped with a defibrillator) and in whom no symptoms of organic heart disease have been found by any means including cardiac catheterization

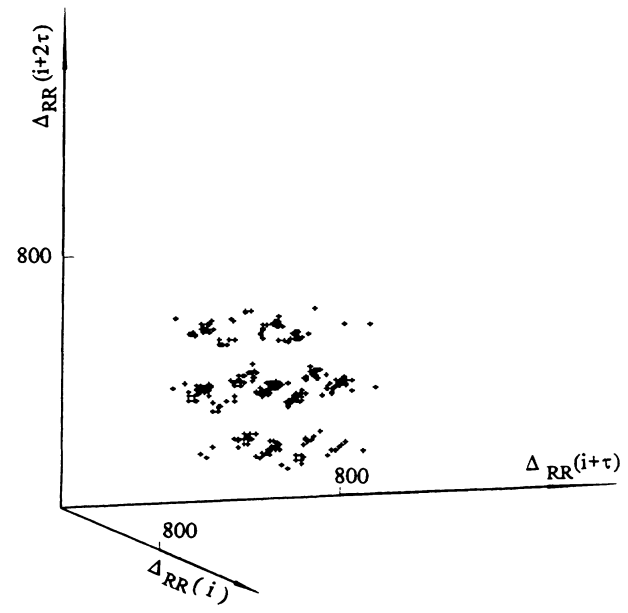

FIG. 6. Image of a highly ordered state (patient C.G.N.) which lasted for about 50 min and was succeeded by an asystole.

and biopsy. C.H.M. is a healthy individual and a medically matched control for B.H.D. The smooth curve in these figures and all similar figures below depicts the cumulative entropy, while the strongly oscillating curve depicts the window entropy. The large dip seen in Fig. 8(a) in window entropy occurred when the patient C.H.M. went through an exercise stress test. Although the details of the curves differ, it should be stressed that the overall characteristics of the two cases are remarkably similar: the minimum of cumulative entropy for C.H.M. (2.64) is slightly larger than for B.H.D. (1.52). The average and the maximum in both cases correspond well (2.7 versus 3.11 and 3.06 versus 3.03, respectively). The same holds true for window entropy in both these cases.

A second example is given in Fig. 10, which depicts the first 4 h of the window and cumulative entropies of the case of D.W.D.1, and in Fig. 11, where the same is presented for D.W.D.3. These figures depict the first 4 h of entropy curves for the same patient 18 h before and 1 yr after cardiac arrest. Thus D.W.D.3 is the control for D.W.D.1. Although the 24-h return maps for these two examples differ greatly (Fig. 3), one-dimensional entropy

TABLE I. Entropy of *RR* intervals for cardiac arrest and for sex, age, and disease matched controls.

	Average	Maximum	Minimum
	Cumulative entropy		
Cardiac arrest	2.48±0.62	2.94±0.31	1.79±0.47
	$p=0.1$	$p=0.2$	$p=0.08$
Controls	2.72±0.25	3.05±0.25	2.01±0.42
	Window entropy		
Cardiac arrest	1.94±0.42	3.14±0.4	0.867±0.34
	$p=0.3$	$p=0.14$	$p=0.15$
Controls	2.02±0.28	2.96±0.28	1.00±0.22

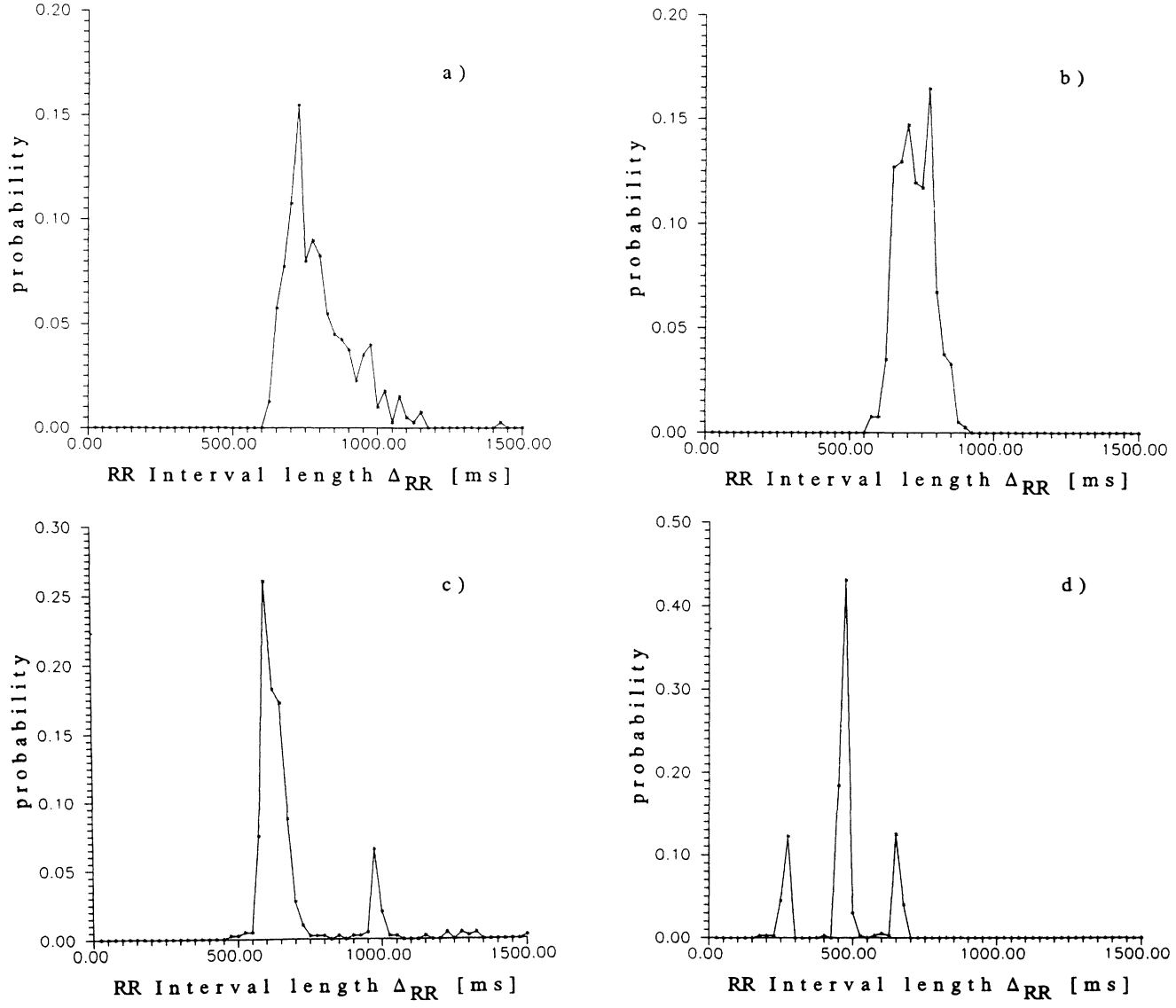

FIG. 7 Examples of histograms of 400-beat-long *RR* interval sequences measured at different moments in time for (a) and (b) the healthy individual C.H.M. and (c) and (d) C.G.N.

Eq. (1) seems to be as poor a tool to distinguish between medically different situations as is the total entropy of the whole 24-h *RR* sequence. The maximum of S_w for D.W.D.1 was 2.659, its average in the 24 h was 2.236, and its minimum was equal to 1.256. For D.W.D.3, the respective values were 3.012, 2.730, and 1.832. D.W.D. was, however, perhaps one of the most extreme cases we have studied so far. Table I gives the following data for

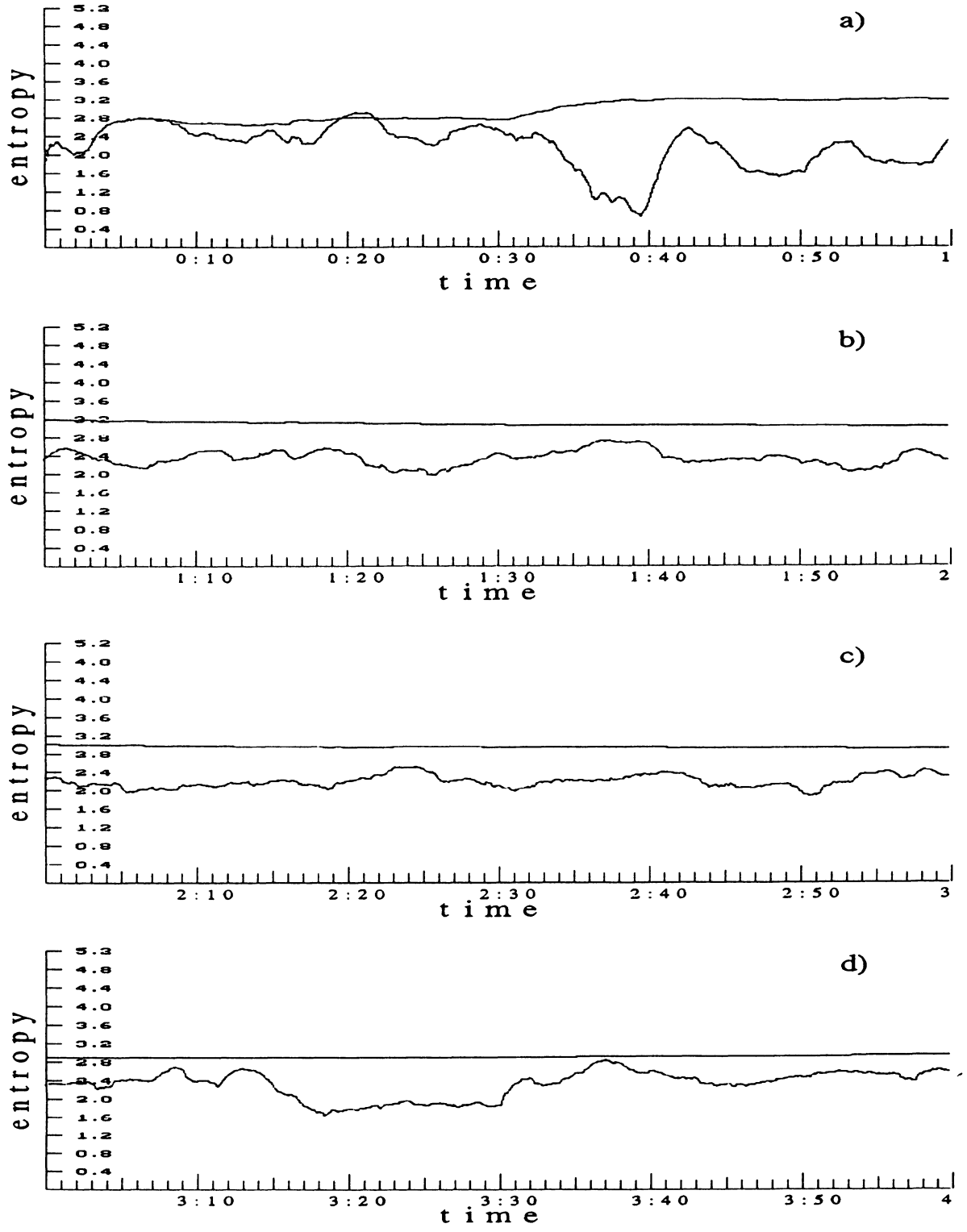

FIG. 8. The first 4 h of the window entropy (oscillating curve) and the cumulative entropy (smooth curve) as functions of time for the healthy individual C.H.M.

all ten cardiac arrest cases and sex, age, and disease status matched controls: the 24-h average value and the maximum and the minimum for each recording averaged over the whole group are given with their standard deviation. p denotes the paired t-student test correlation coefficient. For the correlation to be significant p should be less than 0.05. From the data in Table I and Figs. 8–11 it is clear that, on the basis of one-dimensional entropy—cumulative and window alike—it would be difficult to be sure which type of case one is analyzing.

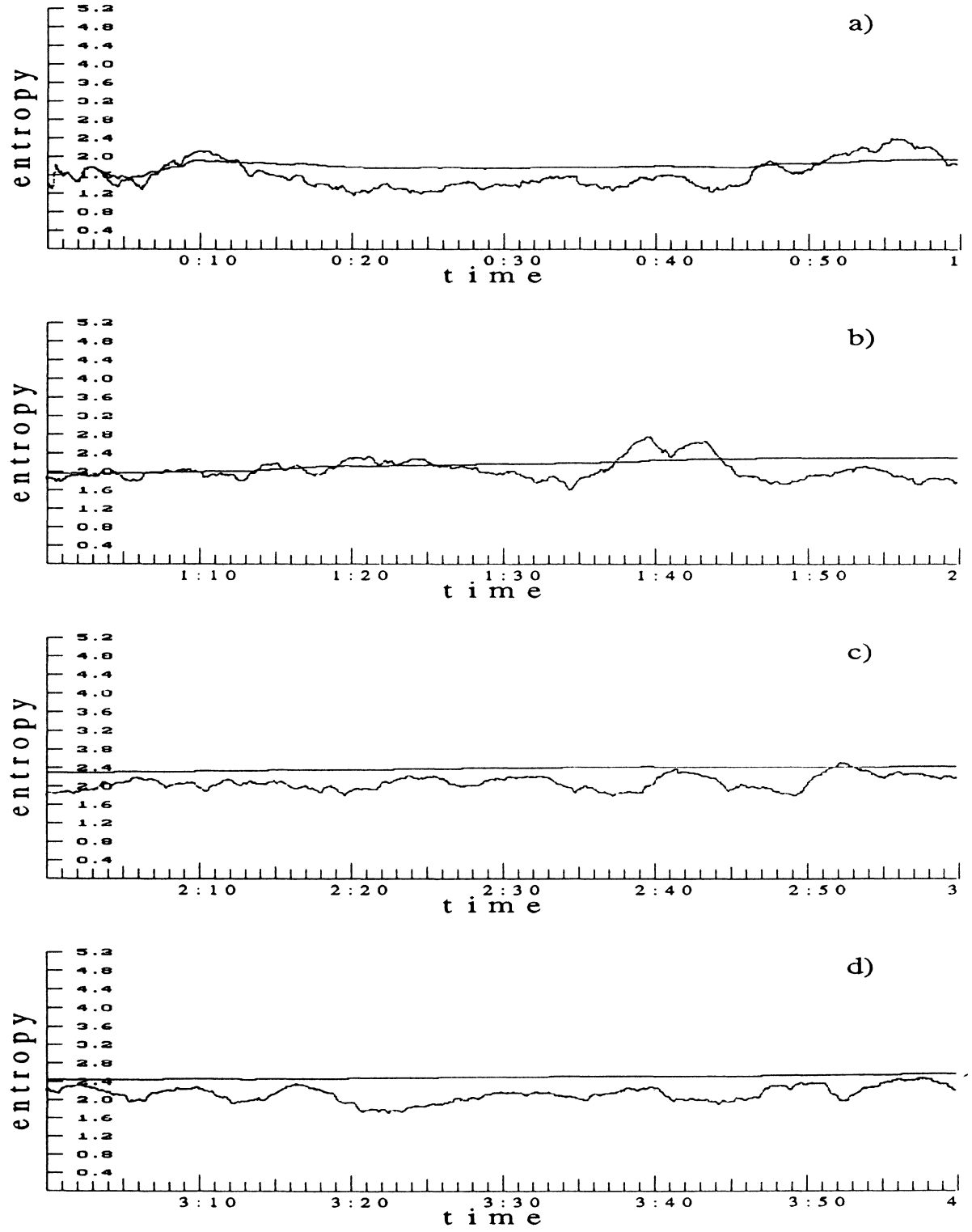

FIG. 9. The first 4 h of the window entropy (oscillating curve) and the cumulative entropy (smooth curve) as functions of time for the patient B.H.D. The control of B.H.D. is C.H.M. (Fig. 8).

V. PATTERN ENTROPY

A. Definition and properties

To have the advantage of using two- and three-dimensional images of *RR* intervals a pattern entropy was defined,

$$S_p = -\sum_{k=1}^{N} p_k \ln p_k, \tag{2}$$

with p_k defined for two dimensions as

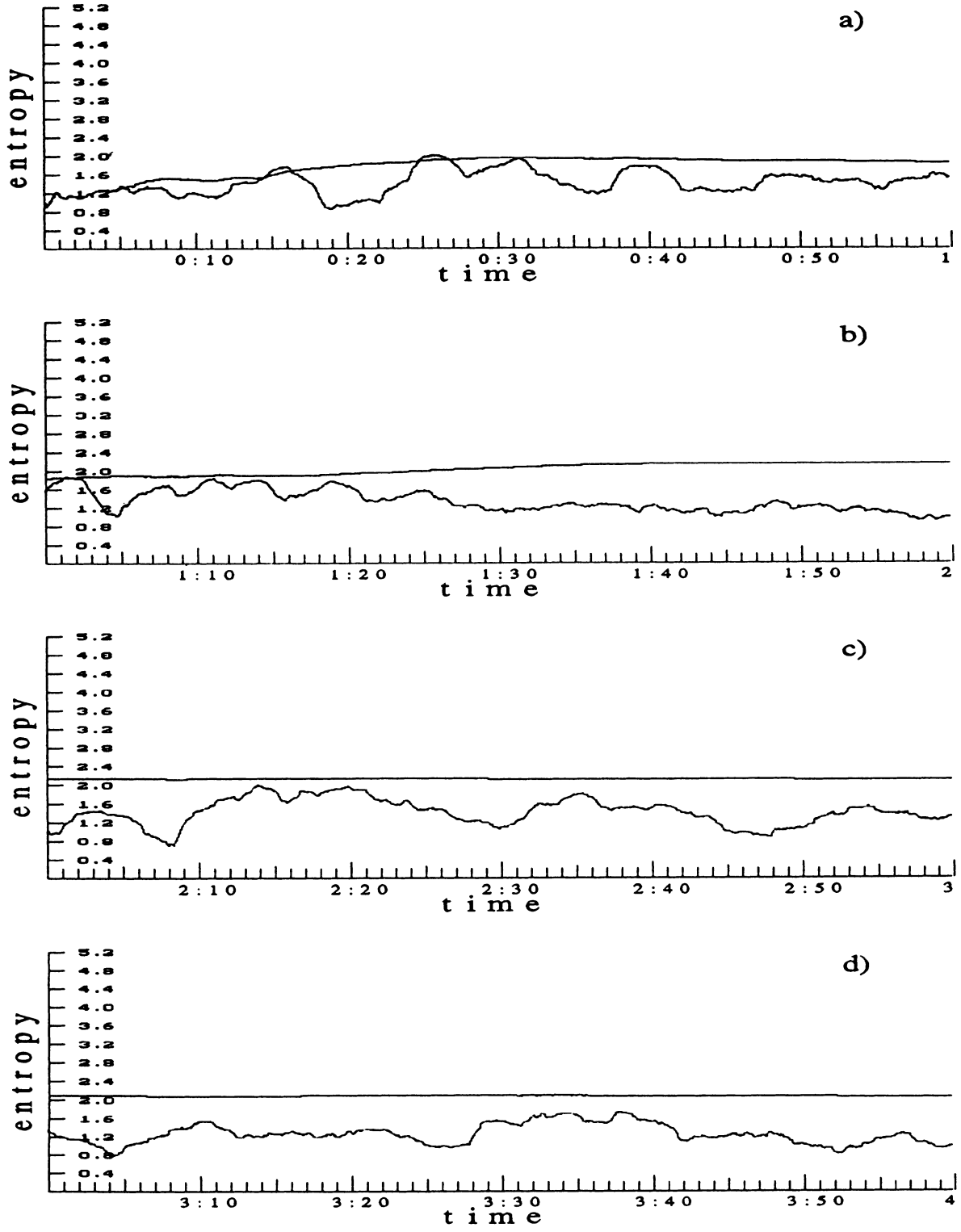

FIG. 10. The first 4 h of the window entropy (oscillating curve) and the cumulative entropy (smooth curve) as functions of time for the patient D.W.D. before cardiac arrest.

$$p_k = p(\Delta_{RR}) p_\tau(\Delta_{RR})$$

and for three dimensions as

$$p_k = p(\Delta_{RR}) p_\tau(\Delta_{RR}) p_{2\tau}(\Delta_{RR}) ,$$

where τ is the integer time delay in beats and p denotes the probability of finding a given length Δ_{RR} in the sequence of RR intervals ending at some interval index i, as described for Eq. (1). p_τ and $p_{2\tau}$ are found similarly, but for different sequences of RR intervals, namely, those

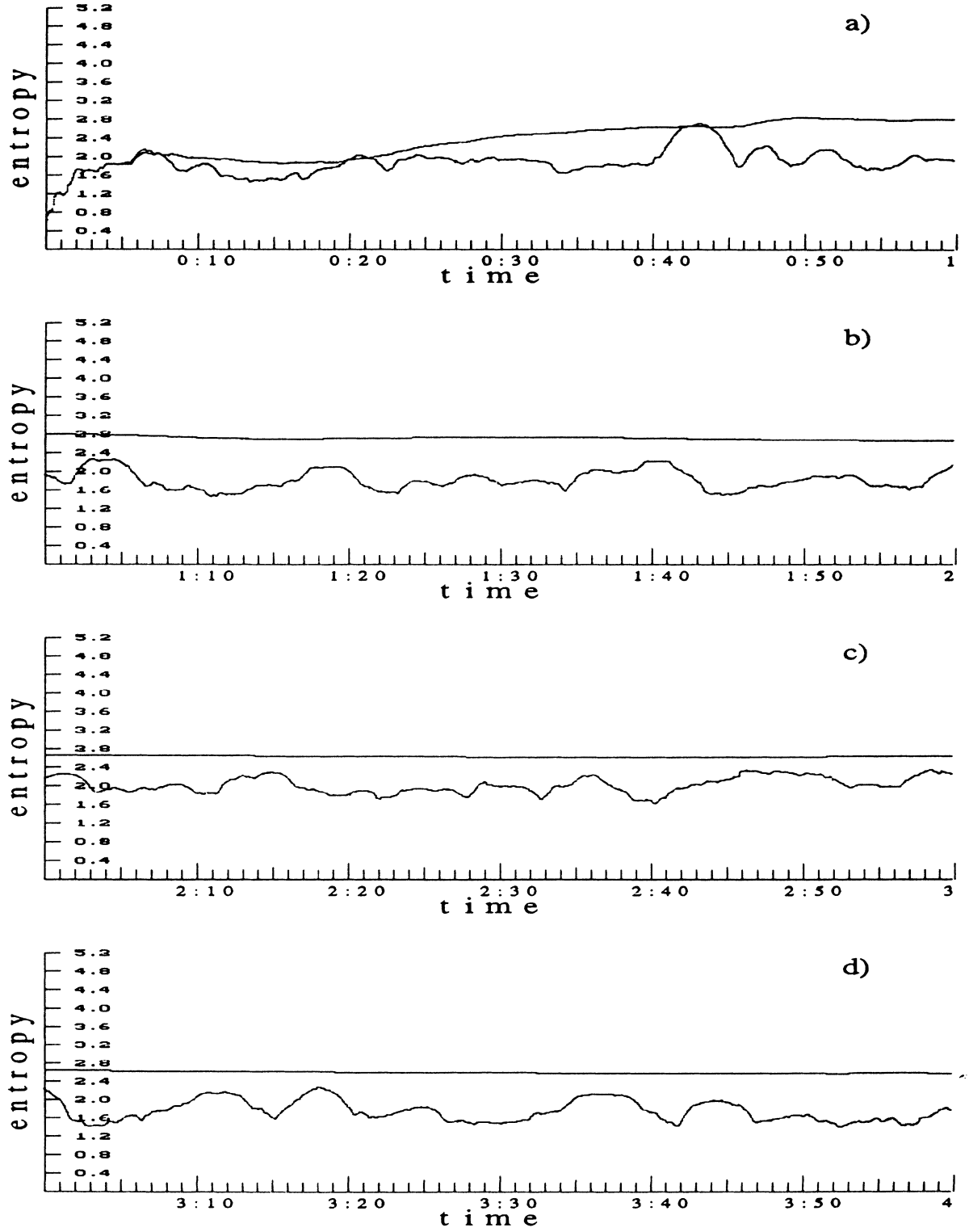

FIG. 11. The first 4 h of the window entropy (oscillating curve) and the cumulative entropy (smooth curve) as functions of time for the patient D.W.D. 1 y after cardiac arrest.

which end at the interval indices $i+\tau$ and $i+2\tau$, respectively. p_k is thus obtained by multiplying the simple probabilities calculated for each delay coordinate separately. Because the joint probability p_k is a very small quantity, for ease of use, we multiplied all pattern entropies by 10^4.

The main idea in defining entropy in this way was to find a quantitative measure to distinguish between the dynamics of ordered heart action such that the probability distributions obtained from the data without a time shift and those for the data shifted in the time by τ and 2τ would differ very little [then the joint probability of Eq. (2) would be large] and such that the probability distribution of the *RR* interval lengths changes rapidly with the time so that the joint probability is small. Note that because joint probability is used here, *pattern entropy will have the peculiar property that it will be large for processes which are well ordered and stationary in the time, while small otherwise.*

Figure 12 depicts the cumulative (flat curve) and the window pattern entropy (wavy curve) as functions of the time for the first hour of the recording for a healthy individual [C.H.M., cf. Fig. 1(b)] for different values of the delay τ. It can be seen that, for the first 9 min, the two quantities have practically the same value as the difference between the time window length and the current time value is small. The window pattern entropy curve as a function of the time undulates slowly. The sharp rise in the value of this entropy between 32 and 42 min is due to an exercise stress test—an effect due to an ordering of the dynamics of the system at that time. It should be stressed at this point that pattern entropy is not a simple function of the standard deviation of the *RR* intervals within the given time window. We noted numerous instances, during stress tests and at other moments in time for unknown reasons, when the three-dimensional map time window image was contracted to a small island and yet, instead of increasing sharply, the value of the window pattern entropy dropped suddenly, indicating a disordering of the *RR* interval sequence.

Consecutive points in the *RR* interval sequence are one whole cycle of the system away on the time scale; thus a delay of one heartbeat ($\tau=1$) may be considered rather long when measured in real time. As mentioned above, for optimal imaging effect three-dimensional *RR* interval return maps were observed here with $\tau=2$. This does not mean, however, that the same delay time has to be the best for pattern entropy calculations. The effect of the change of the length of the delay τ from 25 [Fig. 12(a)] to 200 heartbeats [Fig. 12(d)] with the length of the time window held constant at 400 beats (equivalent for this recording to between 3.5 and 5.2 min of real time) is very weak. It can be seen that only when the delay time exceeds 50% of this rather long time window does the shape of the window pattern entropy as a function of the time change significantly. Even then the main features of the curve as seen in Fig. 12(a) are still well recognizable in Fig. 12(d). This indicates that the *RR* interval histograms contain highly persistent features (*RR* interval lengths which are much more probable than others). This may be taken as strong evidence of the deterministic nature of the system. Long range correlations were also found in the ECG signal by Peng *et al.* [2] by completely different means.

The same behavior of pattern entropy as a function of the time was obtained when the length of the time window was changed from 50 to 200 beats and the delay τ held constant at 2 (Fig. 13). A further change of the window length from 200 to 400, except for some further averaging, did not introduce a significant change into the shape of the curves. It can be seen that for the shortest time window one may sensibly use (50 beats), the pattern entropy curve contains many details which are missing from the 100-beat-long window calculation. The analysis of these fine details is a painstakingly long process and the results will be presented separately when a good comparison with the respective three-dimensional *RR* interval map images has been concluded. Both the observation of three-dimensional images of *RR* interval maps within the 50-beat time window and the form of the definition Eq. (2) indicate that the rapid changes of the window pattern entropy seen in Fig. 13(a) are due most of all to recurrent changes in the degree of the ordering of the *RR* interval sequence. Note that if this effect were predominately due to the changes in the value of the standard deviation of *RR* intervals, then the one-dimensional entropy (1) would a have proven to be a much better analysis tool. Increasing the window length averages out some of the detailed features of the window pattern entropy as a function of the time. The main features of the curves in Fig. 13(b) (time window length 100) are seen in Fig. 13(c) for a window which is twice as long [cf. also Fig. 16(a)]. This is again a manifestation of the persistent features of the *RR* interval histograms: some interval lengths are much more probable than others. In fact, inspection of the probability distribution of *RR* intervals (i.e., their histogram) and of the distribution squared and then cubed shows that the calculation of a momentlike quantity such as that used in Eq. (2) has the effect of enhancing the size of the peaks in the distribution with respect to the rest of the distribution (Fig. 14; all histograms shown have been renormalized to 1 for ease of comparison).

We note here, but do not elaborate, that the same main results were obtained when the time window was set to 50 and the delay was changed from 2 to 50. Again, only after the delay exceeded 50% of the window length did the shape of the curves as a function of the time change significantly, but the main features of the curves were retained.

B. Application to medical diagnosis

Figure 15 depicts the first 4 h of the dependence of cumulative (smooth curve) and window pattern entropy (jagged curve) on the time for the patient B.H.D., who has undergone several cardiac arrests, but whose heart condition examined by all means (including frequency domain analysis, catheterization, and biopsy) seems otherwise completely normal. These same quantities for the sex, age, and disease matched control pair of B.H.D.—patient C.H.M.—are shown in Fig. 16. The one-dimensional entropy as a function of the time for these

two cases was discussed above (Figs. 8 and 9). In Fig. 15 it can be seen that cumulative pattern entropy is a slowly decreasing function of time while window pattern entropy oscillates between 700 and 2200 (arbitrary units). In Fig. 16 it can be seen that the cumulative entropy for the healthy matched control C.H.M. is practically a constant on the level of about 400 (except for the first 35 min when the statistics are still poor). It should be stressed at this

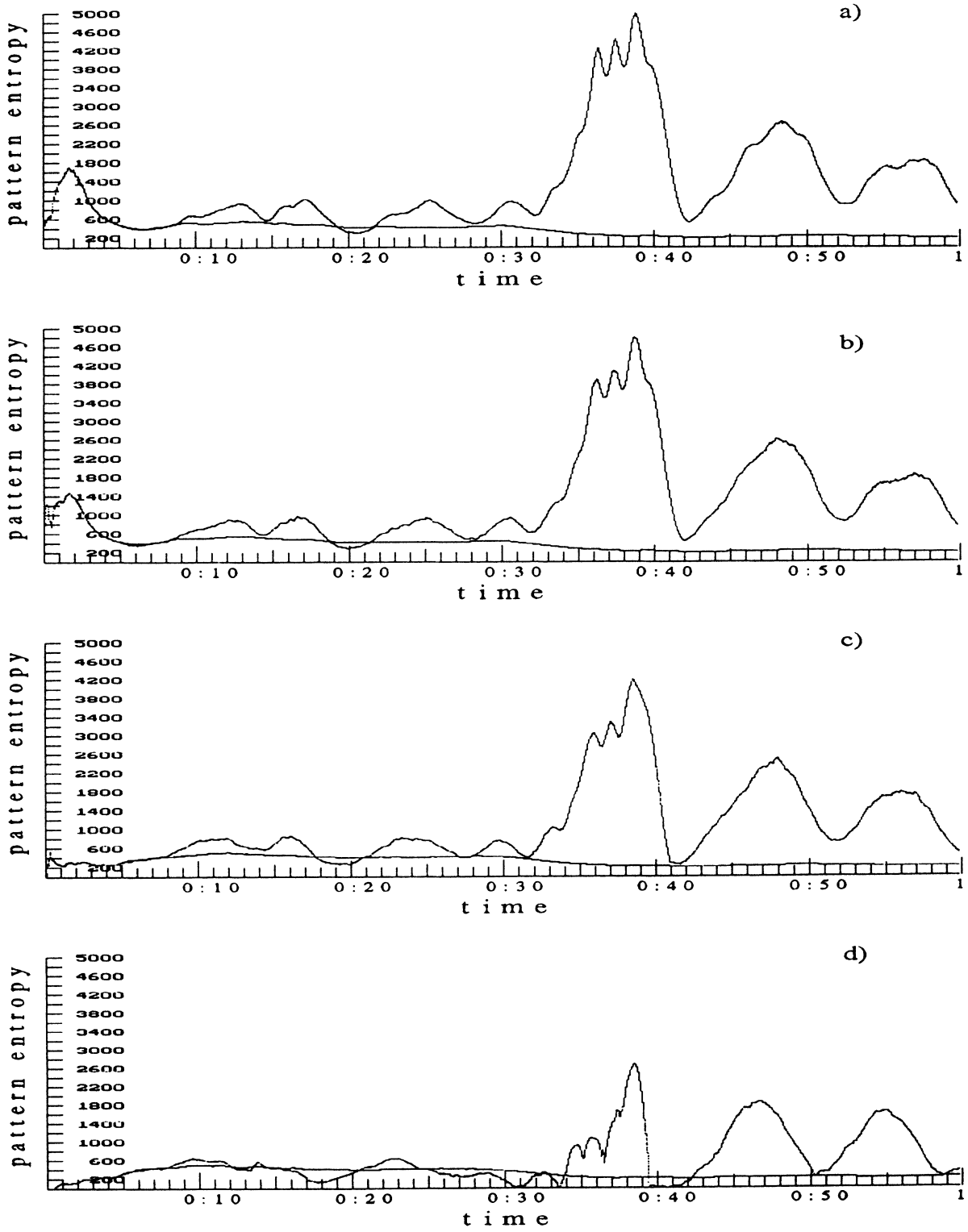

FIG. 12. The first hour of the window pattern entropy (oscillating curve) and the cumulative pattern entropy (smooth curve) as functions of time for the patient C.H.M. and for the 400-beat-long time window with $\tau=25$ (a), 50 (b), 100 (c), and 200 (d).

point that, in sharp contrast to the one-dimensional entropies, viewed in the pattern entropy picture, the two members of the matched pair differ greatly. Apart from the period of time between 32 and 42 min [Fig. 16(a)] when the C.H.M. went through an exercise text (cf. also Figs. 8 and 13), window pattern entropy for this case has a lower amplitude of oscillations and a lower average than for the severely ill member of the matched pair B.H.D. (Fig. 15). Cumulative entropy for B.H.D. appears to be significantly higher than for C.H.M.: the 24-h average is equal to 601 versus 295, respectively. The most striking difference between members of a given matched pair is seen when the value of the maximum within the 24-h recording of the cumulative pattern entropy is compared. For the pair B.H.D. and C.H.M. the values were 3259 versus 561, respectively. All these differences noted in the curves in Figs. 15 and 16 indicate that, in a healthy individual, the degree of ordering is lower than for the cases of pathology studied here. In general, in the latter case the degree of ordering (window pattern entropy) has a much larger amplitude of change. Such differences were typical for other sex, age, and disease matched pairs examined. Another good example of this is shown in Figs. 17 and 18 where the first 4 h of two Holter recordings of the same patient D.W.D. taken 18 h before cardiac arrest and 1 y after it, respectively, are examined by means of pattern entropy. The same data are also presented in Figs. 10 and 11 in the one-dimensional entropy image and in Fig. 3 in a global, 24-h form. It can be seen that the average and the amplitude of window pattern entropy for the case before cardiac arrest (Fig. 17) are much larger than when this patient has been brought back to a more normal state of health (Fig. 18). Also, cumulative pattern entropy is much

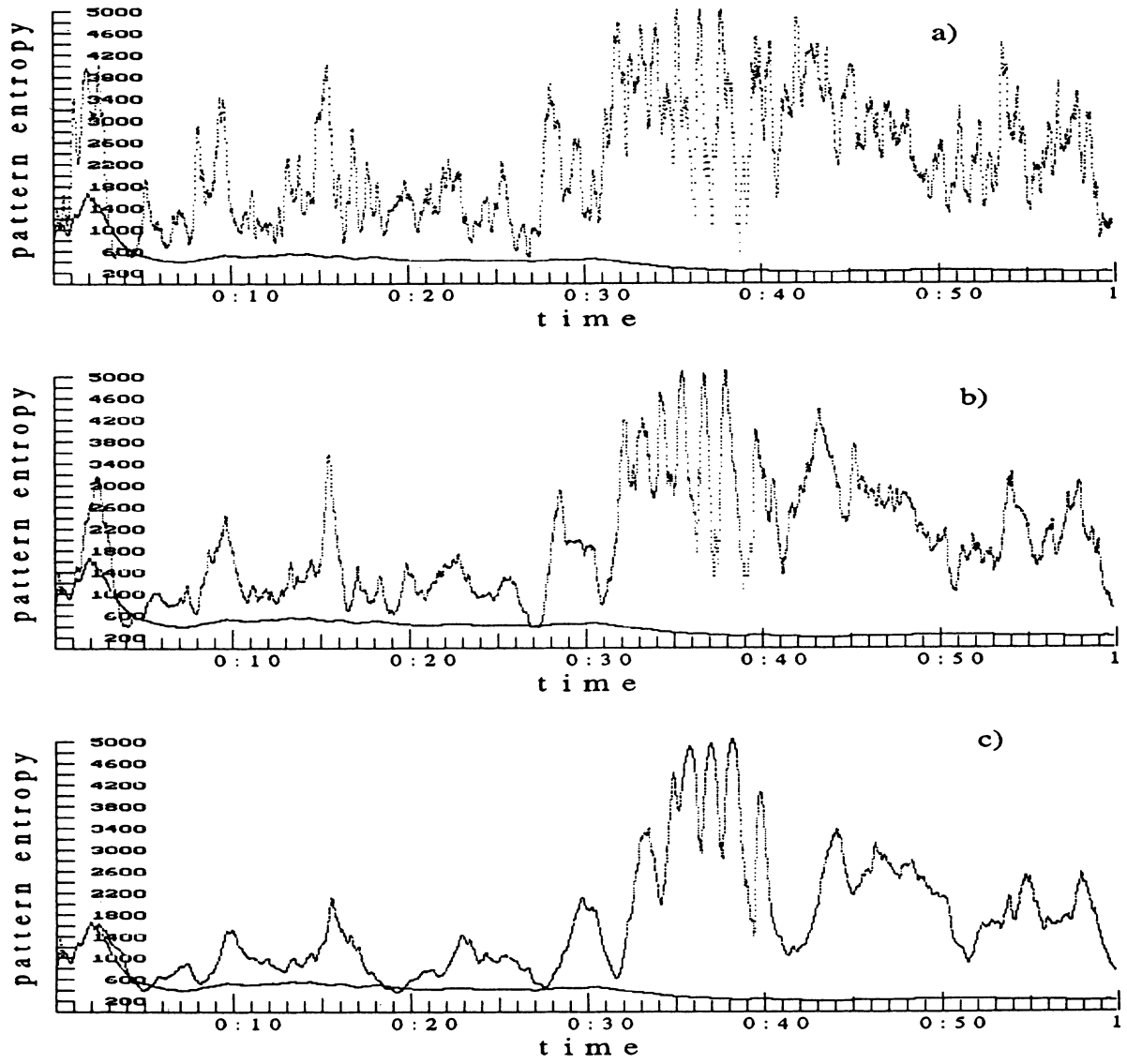

FIG. 13. The first hour of the window pattern entropy (oscillating curve) and the cumulative pattern entropy (smooth curve) as functions of time for the patient C.H.M. and for $\tau=2$ and a window length of (a) 50, (b) 100, and (c) 200 beats.

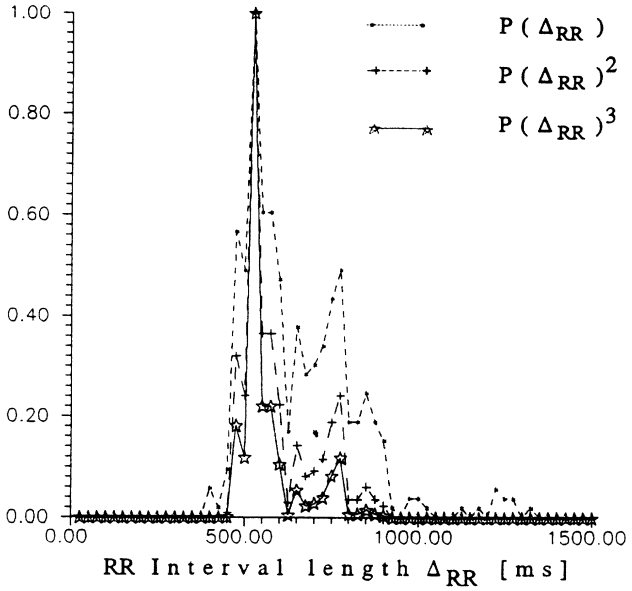

FIG. 14. An example of the probability density of *RR* interval lengths $p(\Delta_{RR})$ taken to the first, second, and third power. All probability density distributions shown have been renormalized to 1 for ease of comparison.

lower in the latter case. The 24-h averages of the window pattern entropy and cumulative pattern entropy for the cardiac arrest cases examined here versus sex, age, and disease matched controls are presented in Table II. It can be seen that the paired *t*-test correlation coefficient *p* is much lower than 0.05 for the average and for the maximum cumulative pattern entropy as well as for the maximum of window pattern entropy. Thus these quantities differentiate well between the cardiac arrest cases and their matched controls.

Pattern entropy seems to differentiate also between groups with a high and a low risk of cardiac arrest. It is extremely large for patients who subsequently died, experienced recurrency of cardiac arrest, or had their arrhythmic events when wearing the Holter device (1253 versus 608 24-h average cumulative pattern entropy). When confirmed by future extensive studies the finding presented here should be of real importance as an alternative measure of the cardiological risk factor.

TABLE II. Pattern entropy of *RR* intervals for cardiac arrest cases and matched controls.

	Average	Maximum	Minimum
	Cumulative pattern entropy		
Cardiac arrest	814±468	2332±952	419±231
	$p=0.05$	$p=0.003$	$p=0.07$
Controls	568±199	1389±560	299±101
	Window pattern entropy		
Cardiac arrest	2012±832	4429±648	307±141
	$p=0.1$	$p=0.03$	$p=0.3$
Controls	1692±484	3986±432	337±129

VI. SUMMARY AND CONCLUSIONS

RR interval sequences extracted from 24-h Holter ECG recordings were examined in the framework of nonlinear dynamics. Using the theorem of Takens on phase space trajectory reconstruction in embedding space, three-dimensional images of the return maps $\Delta_{RR}(i+2\tau)$ versus $\Delta_{RR}(i+\tau)$ and $\Delta_{RR}(i)$ were formed for data taken both from healthy subjects and from members of the highest cardiological risk group. It was found that, when viewed with a time window and with a judiciously chosen delay time τ, sequences of *RR* intervals form characteristic shapes in phase space. These shapes generally fall into two basic groups dubbed by us radial and spiral behavior. Although spiral behavior was found to dominate in healthy individuals and radial behavior occurs often in cases of various pathology (e.g., arrhythmia), both types of *RR* sequence dynamics may occur in recordings of any individual. Bifurcations are then often observed between the two types of *RR* sequences. Intermittency may also occur. In some cases of severely ill persons a bifurcation occurs to a state with well defined frequencies which appears in the three-dimensional return map image as isolated islands of points.

As the basic goal of this research was to find a physical tool for medical diagnostics of the heart rate dynamics and that goal was not to be attained by inspection of the *RR* interval return maps alone, a quantitative measure was sought which would be sufficiently local in the time not to be sensitive to the inherent nonstationarity of the ECG signal. A simple calculation of the entropy of the *RR* sequences [Eq. (1)] based on the measured probability distribution of the intervals—whether as cumulative entropy calculated from the beginning of the recording to the given moment in time or as window entropy calculated within a time window—failed to differentiate in any way between healthy and ill individuals. This was true both for individual medically matched pairs and for the whole group of cardiac arrest cases and their sex, age, and disease matched controls.

As an alternative quantitative measure, pattern entropy [Eq. (2)] of the three-dimensional return maps constructed from the 24-h *RR* sequence was defined using a joint probability that the same *RR* interval length occurs in the original $\Delta_{RR}(i)$ interval sequence and in both sequences $\Delta_{RR}(t+\tau)$ and $\Delta_{RR}(t+2\tau)$, which were shifted by an appropriate multiple of the Takens delay τ. Pattern entropy was defined in two forms: as the cumulative and the window pattern entropies.

In general, pattern entropies of both types as functions of time are extremely robust both against the choice of window length and against the choice of the exact delay τ. This is seen as a strong indication that some *RR* interval lengths are much more probable than others (persistent, so to speak) and that this is a clear indication of

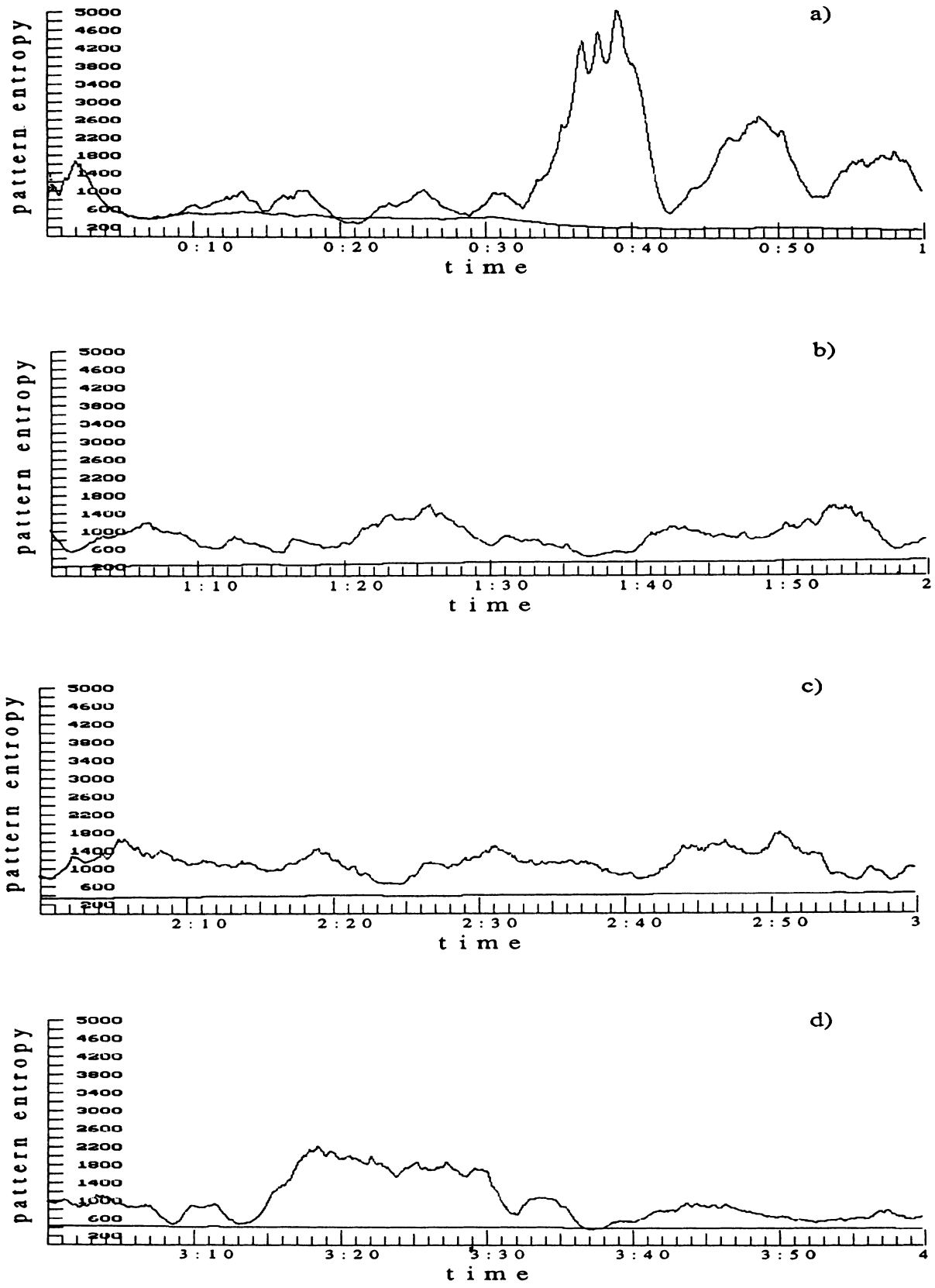

FIG. 15. The first 4 h of the window pattern entropy (jagged curve) and the cumulative pattern entropy (smooth curve) as functions of time for the control C.H.M.

the determinism of the system or systems controlling heart action.

In the limit of large time window length (400 beats) and small delay time ($\tau=2$), it was found that the maximum of the window pattern entropy and the maximum of the cumulative pattern entropy as well as their time averages within the 24-h recording are quantities which correlate surprisingly well with the state of health of the

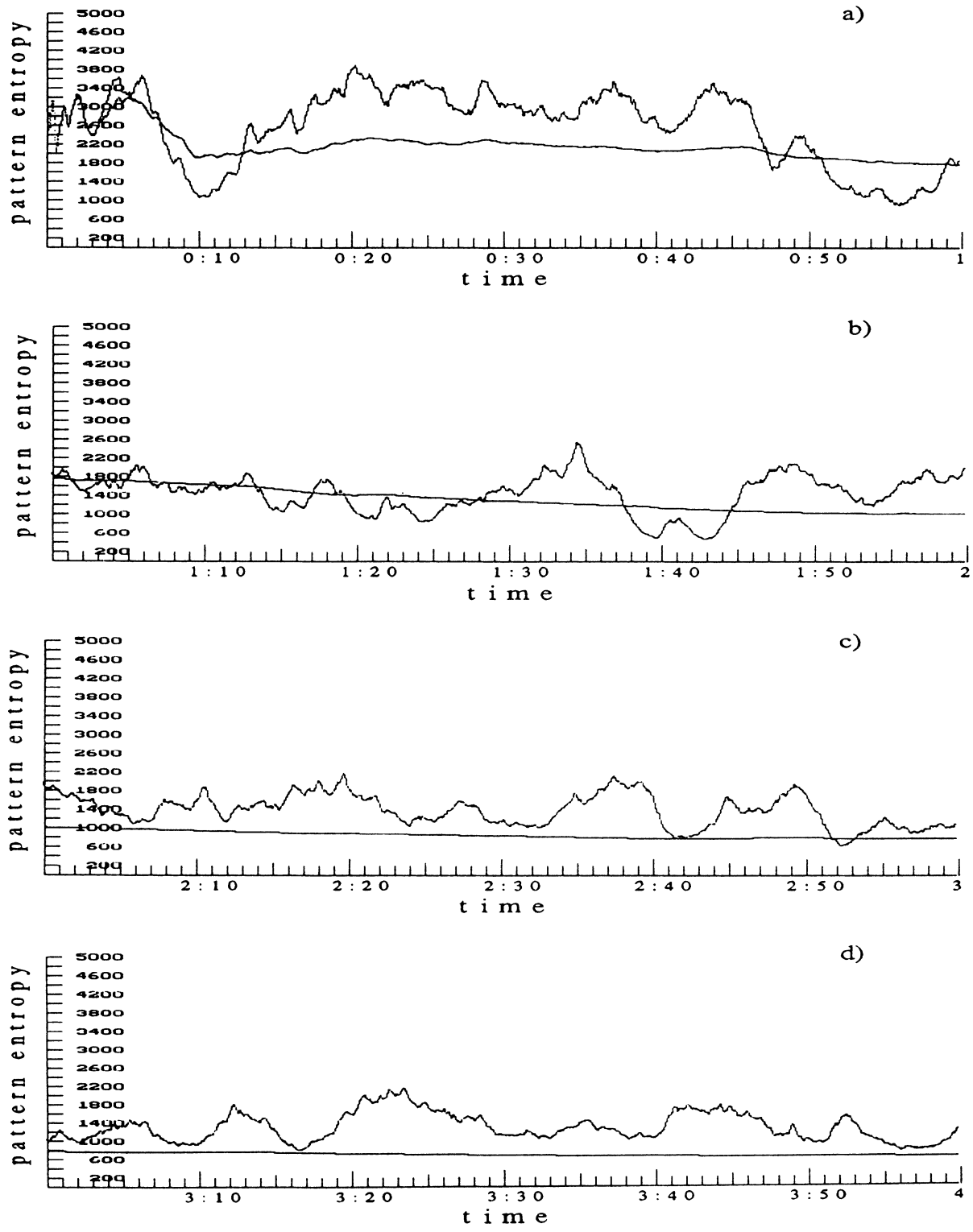

FIG. 16. The first 4 h of the window pattern entropy (jagged curve) and the cumulative pattern entropy (smooth curve) as functions of time for the patient B.H.D. whose control is C.H.M. (Fig. 15).

person studied. The statistical data presented here pertain to cases of a high risk of cardiac arrest and their age, sex, and disease matched controls. As an aside, we mention that the levels of pattern entropy measured in the *RR* sequences of cardiomyopathic patients has been shown—in a much more medically oriented study to be presented separately—to correlate very well with levels of a cardiacally critical hormone—noradrenaline.

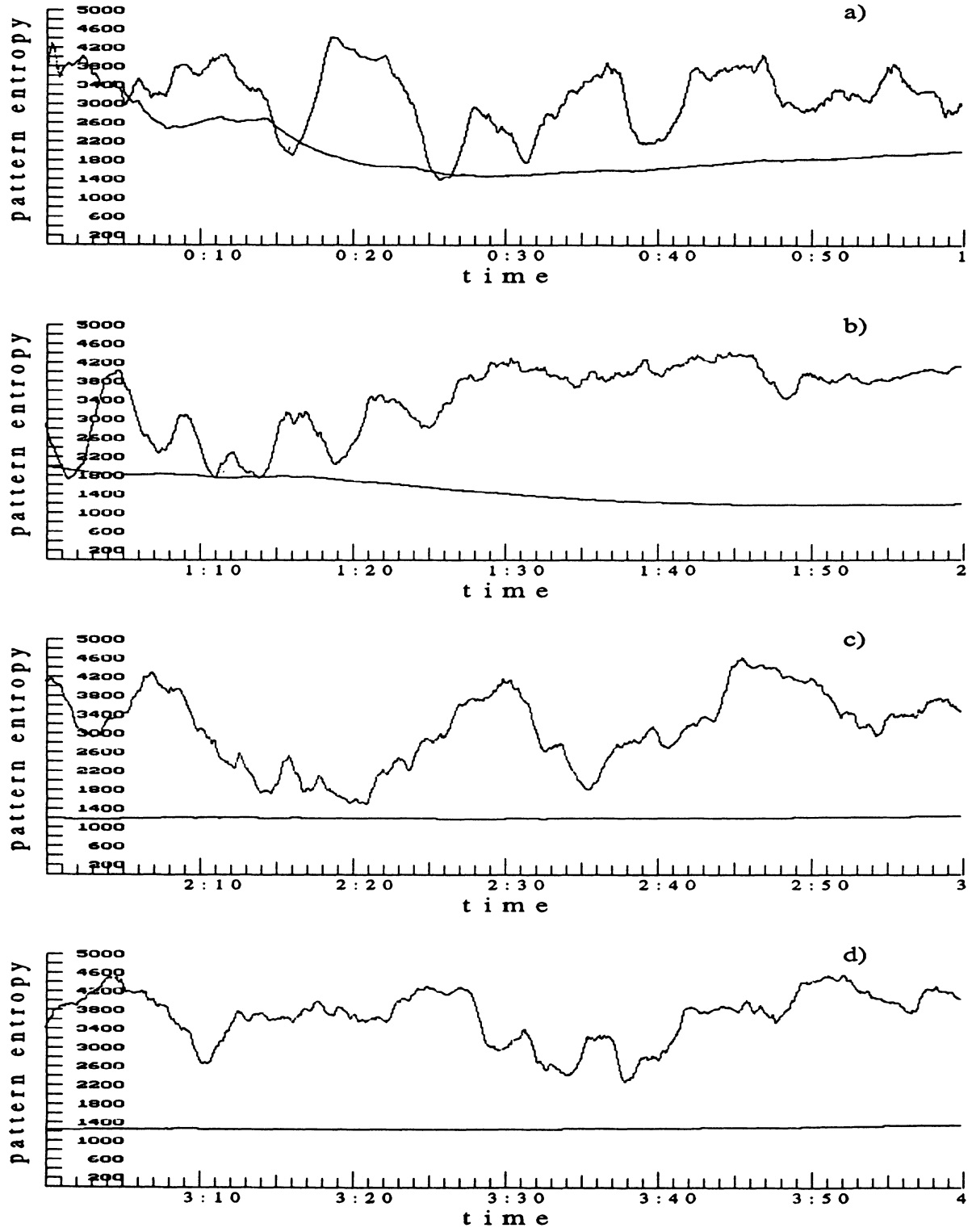

FIG. 17. The first 4 h of the window pattern entropy (jagged curve) and the cumulative pattern entropy (smooth curve) as functions of time for the patient D.W.D. before cardiac arrest.

To conclude, a simple to calculate, robust and insensitive to both nonstationarity and artifacts, nonlinear dynamical tool—pattern entropy—has been found which is able to differentiate between different types of cardiological dynamics. In particular, pattern entropy is able to discern between illness and health also in those cases where other cardiological diagnostics of heart rate variability fail.

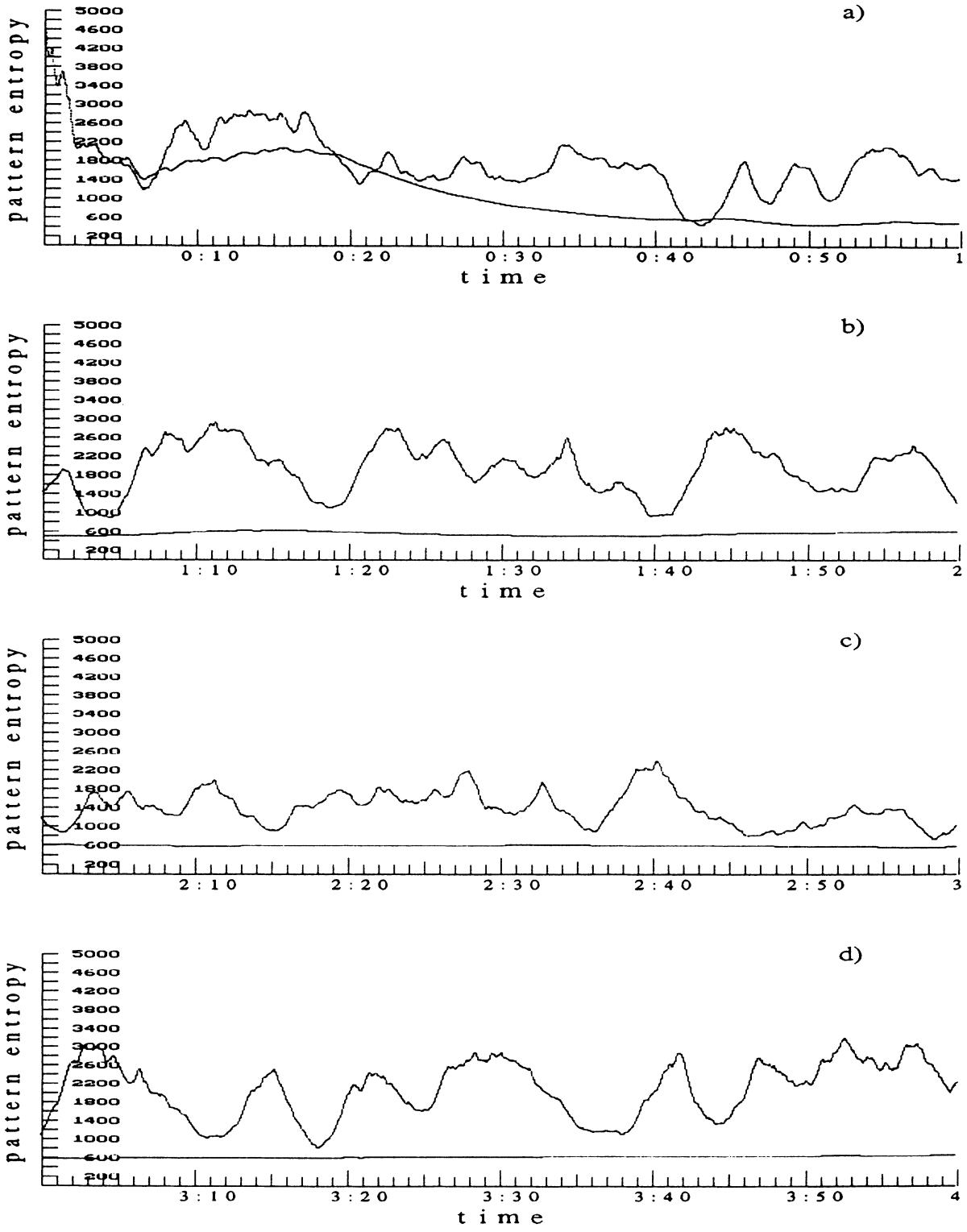

FIG. 18. The first 4 h of the window pattern entropy (jagged curve) and the cumulative pattern entropy (smooth curve) as functions of time for the patient D.W.D. 1 y after cardiac arrest.

ACKNOWLEDGMENTS

Peter Scherer is thanked for providing valuable references to time domain and frequency domain analysis of heart rate variability analysis. This work was financially supported in part by KBH Grant No. 4 1043 91 01 and in part by Research Funds of Warsaw University of Technology.

[1] B. J. West, *Fractal Physiology and Chaos in Medicine* (World Scientific, Singapore, 1990), pp. 208–222.

[2] C.-K. Peng, J. Mietus, J. M. Hausdorf, S. Havlin, H. E. Stanley, and A. L. Goldberger, Phys. Rev. Lett. **70**, 9 (1993); **70**, 1343 (1993).

[3] Y. Yamamoto, R. L. Hughson, J. R. Sutton, C. S. Houston, A. Cymerman, E. L. Fallen, and M. V. Kamath, Biol. Cybern. **69**, 205 (1993).

[4] T. A. Denton, G. A. Diamond, S. S. Khan, and H. Karagueuzian, J. Electrocardiol. Suppl. **24**, 84 (1992).

[5] M. A. Woo, W. G. Stevenson, D. K. Moser, R. B. Trelease, and R. M. Harper, Am. Heart J. **123**, 3 (1992); **123**, 704 (1992).

[6] D. T. Kaplan, J. Electrocardiol. Suppl. **24**, 77 (1992).

[7] J. A. Glazier, M. H. Jensen, A. Libchaber, and J. Stavans, Phys. Rev. A **34**, 1621 (1986); P. Szepfalusy, T. Tel, A. Csordas, and Z. Kovacs, *ibid.* **36**, 3525 (1987).

[8] G. Schmidt, G. Morfill, H. Scheingraber, P. Barthel, H. Kreuzberg, and H. Herb, Proceedings of the XIVth Congress of the European Society of Cardiology [Am. Heart J. Suppl. **123**, 378 (1992)].

[9] J. E. Skinner, C. Carpeggiani, and C. E. Landisman, Circ. Res. **68**, 966 (1991).

[10] M. W. Kroll and K. W. Fulton, J. Electrocardiol. Suppl. **24**, 97 (1992).

[11] R. E. Kleiger, P. K. Stein, M. S. Bosner, and J. N. Rottman, J. Amb. Electrocardiol. **10**, 3 (1992); **10**, 487 (1992).

[12] Zs. Öri, G. Monir, J. Weiss, X. Sayhouni, and D. H. Singer, J. Amb. Electrocardiol. **10**, 499 (1992).

[13] S. M. Pincus, I. M. Gladstone, and R. A. Ehrenkranz, J. Clin. Mon. **7**, 335 (1991).

[14] D. Redington, in *Proceedings of the SPIE Symposium on Chaos in Biology and Medicine*, San Diego, 1993 [Proc. SPIE **2036**, 280 (1993)].

[15] S. P. Reidbord and D. J. Redington, J. Nerv. Ment. Dis. **180**, 649 (1992).

[16] F. Takens, Phys. Rev. Lett. **51**, 14 (1980); **51**, 1265 (1980).

[17] H. G. Schuster, *Deterministic Chaos* (VCH-Verlag, Weinheim, 1988); A. M. Frazer and H. L. Swinney, Phys. Rev. A **33**, 1134 (1986).

[18] A. Goldberger and D. Rigney, in *Theory of Heart: Biomechanics, Biophysics and Nonlinear Dynamics of Cardiac Function* (Springer-Verlag, New York, 1991).